NASA Technical Memorandum 86435

Hypersonic Characteristics of an Advanced Aerospace Plane at Mach 20.3

Ronald S. McCandless

DECEMBER 1985

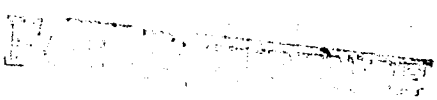

NASA

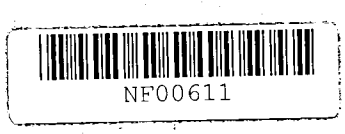

NASA Technical Memorandum 86435

Hypersonic Characteristics of an Advanced Aerospace Plane at Mach 20.3

Ronald S. McCandless
Langley Research Center
Hampton, Virginia

National Aeronautics
and Space Administration

Scientific and Technical Information Branch

1985

SUMMARY

Hypersonic wind-tunnel tests have been conducted at Mach 20.3 in the Langley Hypersonic Helium Tunnel Facility to obtain the static longitudinal and lateral-directional aerodynamic characteristics of an advanced aerospace plane (AAP) concept. Data were obtained at angles of attack (α) from 0° to 25° and at angles of sideslip of -3° and 0°. The test Reynolds number range was 2.5×10^6 to 6.8×10^6 per foot, with the majority of the tests made at 6.8×10^6 per foot. Aerodynamic control effectiveness was determined by deflecting the elevators, the elevons, and the rudder. In addition, a modified canopy was examined for its effects on the vehicle aerodynamics.

Results showed that maximum lift-drag ratio $(L/D)_{max}$ occurred near $\alpha = 12^\circ$ for all control settings tested. With the center of gravity located at 64 percent of the fuselage length, longitudinal stable trim could be achieved for lift-drag ratios near $(L/D)_{max}$. The canopy modification had a negligible effect upon the longitudinal characteristics.

The AAP was shown to be directionally unstable over the angle-of-attack range with positive dihedral effect. Rudder deflection had a negligible effect on the lateral-directional characteristics of the vehicle. Aileron deflection resulted in adverse yaw due to roll control for the test angle-of-attack range.

INTRODUCTION

By the beginning of the next century, it will be technically possible to deploy a vehicle that will be able to leave the atmosphere and fly into low-Earth orbit to perform a mission, fly back into the atmosphere to perform another mission, and then land like a conventional airplane (ref. 1). This advanced aerospace plane (AAP) will be able to provide rapid global response and perform a variety of missions such as reconnaissance, strategic defense, and tactical interdiction.

Because all applications of the AAP will require effective hypersonic operations, a proposed concept has been evaluated in the Langley Hypersonic Helium Tunnel Facility at a Mach number of 20.3. Static stability and control data were obtained over an angle-of-attack range of 0° to 25° for various elevator, elevon, and rudder deflections. In addition, a configuration with a modified canopy was examined. The tests were conducted at unit Reynolds numbers of 2.5×10^6, 3.7×10^6, and 6.8×10^6 per foot. Lateral-directional data were also obtained for angles of sideslip of -3° and 0°. A major goal of this program was to determine the trimmed lift-drag ratio of the vehicle and its stability near the maximum lift-drag ratio.

SYMBOLS AND ABBREVIATIONS

AAP advanced aerospace plane

b wing span, in.

C_A	axial-force coefficient, Axial force/$q_\infty S$
C_D	drag coefficient, Drag/$q_\infty S$
C_L	lift coefficient, Lift/$q_\infty S$
C_l	rolling-moment coefficient, Rolling moment/$q_\infty Sb$
C_{l_β}	rate of change of rolling-moment coefficient with sideslip angle, $\partial C_l/\partial\beta$, deg^{-1}
$C_{l_{\delta_a}}$	rate of change of rolling-moment coefficient with aileron deflection angle, $\partial C_l/\partial\delta_a$, deg^{-1}
$C_{l_{\delta_r}}$	rate of change of rolling-moment coefficient with rudder deflection, $\partial C_l/\partial\delta_r$, deg^{-1}
C_m	pitching-moment coefficient, Pitching moment/$q_\infty Sl$
C_N	normal-force coefficient, Normal force/$q_\infty S$
C_n	yawing-moment coefficient, Yawing moment/$q_\infty Sb$
C_{n_β}	rate of change of yawing-moment coefficient with sideslip angle, $\partial C_n/\partial\beta$, deg^{-1}
$C_{n_{\delta_a}}$	rate of change of yawing-moment coefficient with aileron deflection angle, $\partial C_n/\partial\delta_a$, deg^{-1}
$C_{n_{\delta_r}}$	rate of change of yawing-moment coefficient with rudder deflection, $\partial C_n/\partial\delta_r$, deg^{-1}
C_Y	side-force coefficient, Side force/$q_\infty S$
C_{Y_β}	rate of change of side-force coefficient with sideslip angle, $\partial C_Y/\partial\beta$, deg^{-1}
$C_{Y_{\delta_a}}$	rate of change of side-force coefficient with aileron deflection angle, $\partial C_Y/\partial\delta_a$, deg^{-1}
$C_{Y_{\delta_r}}$	rate of change of side-force coefficient with rudder deflection, $\partial C_Y/\partial\delta_r$, deg^{-1}
c.g.	center of gravity
HHTF	Hypersonic Helium Tunnel Facility
l	model reference length

L/D	lift-drag ratio, C_L/C_D
$(L/D)_{max}$	maximum lift-drag ratio
M	Mach number
p_t	total pressure, psia
q_∞	free-stream dynamic pressure, psia
R_∞	free-stream unit Reynolds number, ft^{-1}
S	planform area, in^2
T_t	total temperature, ^oF
α	angle of attack, deg
β	angle of sideslip, deg
δ_a	aileron deflection angle, $(\delta_{e,L} - \delta_{e,R})/2$, deg
δ_e	total elevon deflection angle, $(\delta_{e,L} + \delta_{e,R})/2$, deg
δ_{el}	elevator deflection angle, deg
$\delta_{e,L}$	left elevon deflection angle, deg
$\delta_{e,R}$	right elevon deflection angle, deg
δ_r	rudder deflection angle, deg

MODEL

The test model was a scaled version of an AAP concept. Figure 1 shows a three-view sketch of the model showing the elevators and elevons in the planform view and the vertical tail and rudder in the side view. The modified canopy is denoted by the dashed lines in the profile and planform views. Positive control deflection conventions are trailing edge down for the elevators and elevons and left for the rudder as viewed from the rear. Elevators were always deflected in the same direction, whereas elevons were deflected symmetrically for longitudinal trim studies and asymmetrically for aileron control studies. All deflections were set by using prebent brackets at 10^o intervals for the elevators and elevons and 15^o intervals for the rudder. The model moment-reference center was set at 64 percent of the body length.

APPARATUS AND TESTS

Wind Tunnel

This investigation was conducted in the 22-inch aerodynamics leg of the Langley Hypersonic Helium Tunnel Facility (HHTF). The HHTF operates in a blowdown mode and

uses purified helium as the test medium at ambient temperature. The test section is approximately 22 inches in diameter, and the test core is 8 to 10 inches in diameter (ref. 2). Flow conditions (including the Reynolds numbers) are given in table I.

Tests

The model was supported on a sting-mounted, six-component, strain-gage balance. Angle of attack was determined by directing light from a high-intensity source to a prism mounted flush with the side of the model and then onto a set of electric eyes. Angle of sideslip was set by applying a fixed amount of yaw to the sting with the model attached. Free-stream flow properties were corrected for real-gas effects in the data reduction program by methods in references 3, 4, and 5. Base pressures were measured at one location, and balance axial forces were adjusted to a condition in which free-stream pressure acted over the model base. More detailed operational and flow characteristics of the HHTF are given in reference 2.

Maximum errors in the data, given in table II, were estimated by using balance accuracies of ±0.5 percent of full-scale design loads. Accuracy of the angles of attack and sideslip was estimated at $\pm 0.1^{\circ}$, and error in the Mach number was estimated at ±0.1.

RESULTS

Longitudinal Characteristics

The longitudinal aerodynamic characteristics for a range of elevator deflections are given in figure 2. The maximum value of L/D occurs at $\alpha = 12^{\circ}$ and varies from 2.48 to 2.60 (fig. 2(a)). Changing elevator deflection had little effect on L/D, with the most notable difference occurring for $\delta_{el} = 20^{\circ}$. For $\alpha \geqslant 12^{\circ}$, the L/D value for δ_{el} was 5 percent lower than the L/D values for other elevator deflections. This reduction in L/D can be attributed to a large increase in axial-force coefficient (fig. 2(c)) and results in a larger drag coefficient, which offsets a smaller percentage increase in lift coefficient (fig. 2(b)).

With the center of gravity located at 64 percent of the body length, deflecting the elevator 10° provides a stable trim point at an angle of attack of 22° with a corresponding L/D value of 2.00 (fig. 2(a)). Extrapolating the pitch data for zero control deflections indicates the configuration would trim near $\alpha = 30^{\circ}$ with a large decrease in L/D. An elevator deflection between 10° and 20° could trim the vehicle at $\alpha = 12^{\circ}$, at which $(L/D)_{max}$ occurs (probably with neutral stability).

Another method to change trim would be to use elevons for additional pitch control. Figure 3 presents the longitudinal characteristics for elevon deflections of 0° and 10° used in conjunction with elevator deflections of 0° and 10°. Figure 3(a) shows that adding an elevon deflection of 10° to the elevator deflection of 10° reduced the angle of attack for trim from 22° to 14° and increased the L/D from 2.00 to 2.50 with approximately the same level of static stability. Also note that the case with $\delta_e = 10^{\circ}$ and $\delta_{el} = 0^{\circ}$ and the case with $\delta_e = 0^{\circ}$ and $\delta_{el} = 10^{\circ}$ had nearly identical pitching-moment coefficient curves. Figures 3(b) and 3(c) show that the case with elevator and elevon deflections of 10° each had larger normal-force and axial-force coefficients at higher angles of attack than the

other cases presented. Larger lift and drag coefficients resulted, especially for $\alpha \geq 12^{\circ}$. Since the percentage increases in lift and drag coefficients were nearly equal, no significant difference in L/D is seen in any of the cases for $\alpha \geq 12^{\circ}$ (fig. 3(a)). There is an increase in L/D at $\alpha < 12^{\circ}$ for the two cases that employ elevon settings, but these data are not as significant as the data for $\alpha \geq 12^{\circ}$, since the vehicle was shown to be untrimmed for all cases at those angles of attack. In general, elevons used in conjunction with the elevators provide adequate trim capability near $(L/D)_{max}$.

A modified canopy configuration was examined for any effects upon the longitudinal aerodynamic characteristics. This modification was a result of peculiar surface flow patterns seen on the leeward surface of the AAP wings during a wind-tunnel test series conducted at the Langley 31-Inch Mach 10 Tunnel. It is thought that the flow from the canopy could be the cause of these flow patterns, which resulted in an anomaly in the axial-force, normal-force, and pitching-moment coefficients at angles of attack between 5° and 10° (ref. 6). Therefore, for completeness, this modified configuration was tested in the HHTF even though the aforementioned anomalies were not evident in the $M = 20$ data presented here. Figure 4 shows that the modified canopy configuration had a negligible effect on the longitudinal aerodynamic characteristics.

Values of C_m and α versus C_N for various elevator, elevon, and combinations of elevator and elevon deflections are given in figure 5 to indicate trim and stability at a center-of-gravity location of 63 percent of the body length, compared with 64 percent. These data indicate that the vehicle can achieve stable trim near $\alpha = 22^{\circ}$ with undeflected controls. Control deflections consisting of either an elevator or an elevon angle setting of 10° could trim the vehicle near $\alpha = 15^{\circ}$ and would result in more desirable flight characteristics than those for the 64 percent center-of-gravity location trim point. By using the present control surfaces and/or changing the center-of-gravity location, the vehicle can be stable and trimmed at angles of attack near $(L/D)_{max}$.

Reynolds number effects on the longitudinal characteristics for the zero controls configuration are presented in figure 6. To obtain the lower Reynolds number data, p_t was reduced, and tunnel blockage conditions were approached at high angles of attack. Therefore, the maximum value of α was limited to 12°. Increasing the Reynolds number reduced the axial-force coefficient (fig. 6(c)) and resulted in an increase in L/D (fig. 6(a)). Normal-force coefficient and lift coefficient were not affected by the changes in Reynolds number.

Lateral-Directional Characteristics

The variations of C_{l_β}, C_{n_β}, and C_{Y_β} with angle of attack for the case with the controls undeflected and for the case with $\delta_{el} = 10^{\circ}$ and $\delta_{e,L} = 20^{\circ}$ are given in figure 7. For these data, positive effective dihedral ($C_{l_\beta} < 0$) is present throughout the test angle-of-attack range except for very small angles of attack ($\alpha < 2^{\circ}$). The vehicle is directionally unstable ($C_{n_\beta} < 0$) over the entire test angle-of-attack range for the two cases shown.

The effects of varying aileron deflection angle on rolling-moment, yawing-moment, and side-force derivatives are given in figure 8 for a total elevon deflection angle of 0°. Roll-control effectiveness ($C_{l_{\delta_a}}$) increased with increasing angle of attack. Increasing the aileron deflection angle from -10° to -20° gave a very slight decrease in $C_{l_{\delta_a}}$. Adverse yaw due to roll control ($C_{n_{\delta_a}} < 0$) was found over the angle-of-attack range, with the aileron deflection angle of -10° producing the most adverse yaw. The ratios of $C_{l_{\delta_a}}$ to $C_{n_{\delta_a}}$ are negative and remained almost constant with increasing angle of attack for $\alpha > 18^{\circ}$.

The effects of varying rudder deflection angle on rolling-moment, yawing-moment, and side-force derivatives are presented in figure 9. As shown, the rudder has a negligible effect on the lateral-directional characteristics over the entire angle-of-attack range.

SUMMARY OF RESULTS

Longitudinal and lateral-directional aerodynamic characteristics of an advanced aerospace plane have been presented at a Mach number of 20.3 over an angle-of-attack range of 0° to 25° and at unit Reynolds numbers of 2.5×10^6, 3.7×10^6, and 6.8×10^6 per foot. The center-of-gravity location was at 64 percent of the fuselage length. The results are summarized as follows:

1. Maximum values of lift-drag ratio ranged from 2.48 to 2.60 and occurred near an angle of attack of 12°.

2. Longitudinally stable trim was achieved near the maximum lift-drag ratio.

3. The modified canopy configuration had a negligible effect on the longitudinal aerodynamic characteristics.

4. The vehicle was directionally unstable over the angle-of-attack range with positive dihedral effect.

5. Aileron deflection studies resulted in adverse yaw due to roll control for all angles of attack.

6. Rudder deflection had no effect on lateral-directional characteristics over the test angle-of-attack range.

NASA Langley Research Center
Hampton, VA 23665-5225
June 18, 1985

REFERENCES

1. Tremaine, S. A.: Air Force Aeronautical Systems - The 1990's: A Major Shift. AIAA-83-2433, Oct. 1983.

2. Arrington, James P.; Joiner, Roy C., Jr.; and Henderson, Arthur, Jr.: Longitudinal Characteristics of Several Configurations at Hypersonic Mach Numbers in Conical and Contoured Nozzles. NASA TN D-2489, 1964.

3. Mueller, James N.: Equations, Tables, and Figures for Use in the Analysis of Helium Flow at Supersonic and Hypersonic Speeds. NACA TN 4063, 1957.

4. Erickson, Wayne D.: Real-Gas Correction Factors for Hypersonic Flow Parameters in Helium. NASA TN D-462, 1960.

5. Maddalon, Dal V.; and Jackson, Willis E.: A Survey of the Transport Properties of Helium at High Mach Number Wind-Tunnel Conditions. NASA TM X-2020, 1970.

6. McCandless, Ronald S.; and Cruz, Christopher I.: Hypersonic Characteristics of an Advanced Aerospace Plane. AIAA-85-0346, Jan. 1985.

TABLE I.- SUMMARY OF TUNNEL TEST CONDITIONS

$p_{t'}$ psia	$T_{t'}$ ^{o}F	M	$R_{\infty'}$ ft^{-1}
327	68	18.3	2.5×10^{6}
517	66	19.1	3.7×10^{6}
1015	66	20.3	6.8×10^{6}

TABLE II.- ESTIMATED ACCURACIES IN MEASURED DATA

Coefficient	Accuracy
C_N	±0.0073
C_A	±0.0020
C_m	±0.0007
C_l	±0.0005
C_n	±0.0005
C_Y	±0.0024

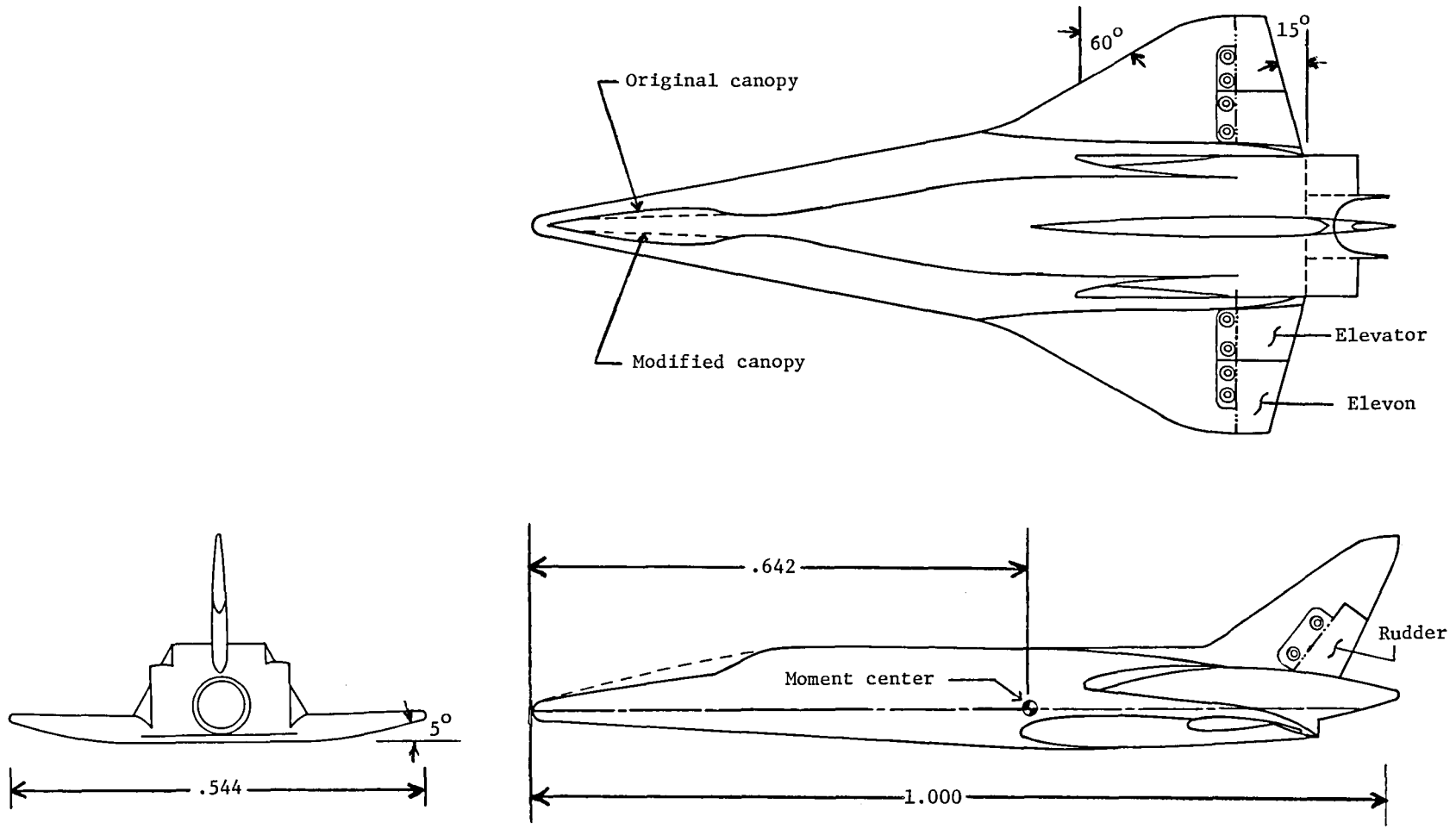

Figure 1.- Sketch of AAP model. Dimensions on figure are normalized by reference length ι. ι = 9.052 in.; S = 16.33 in^2; b = 4.92 in.

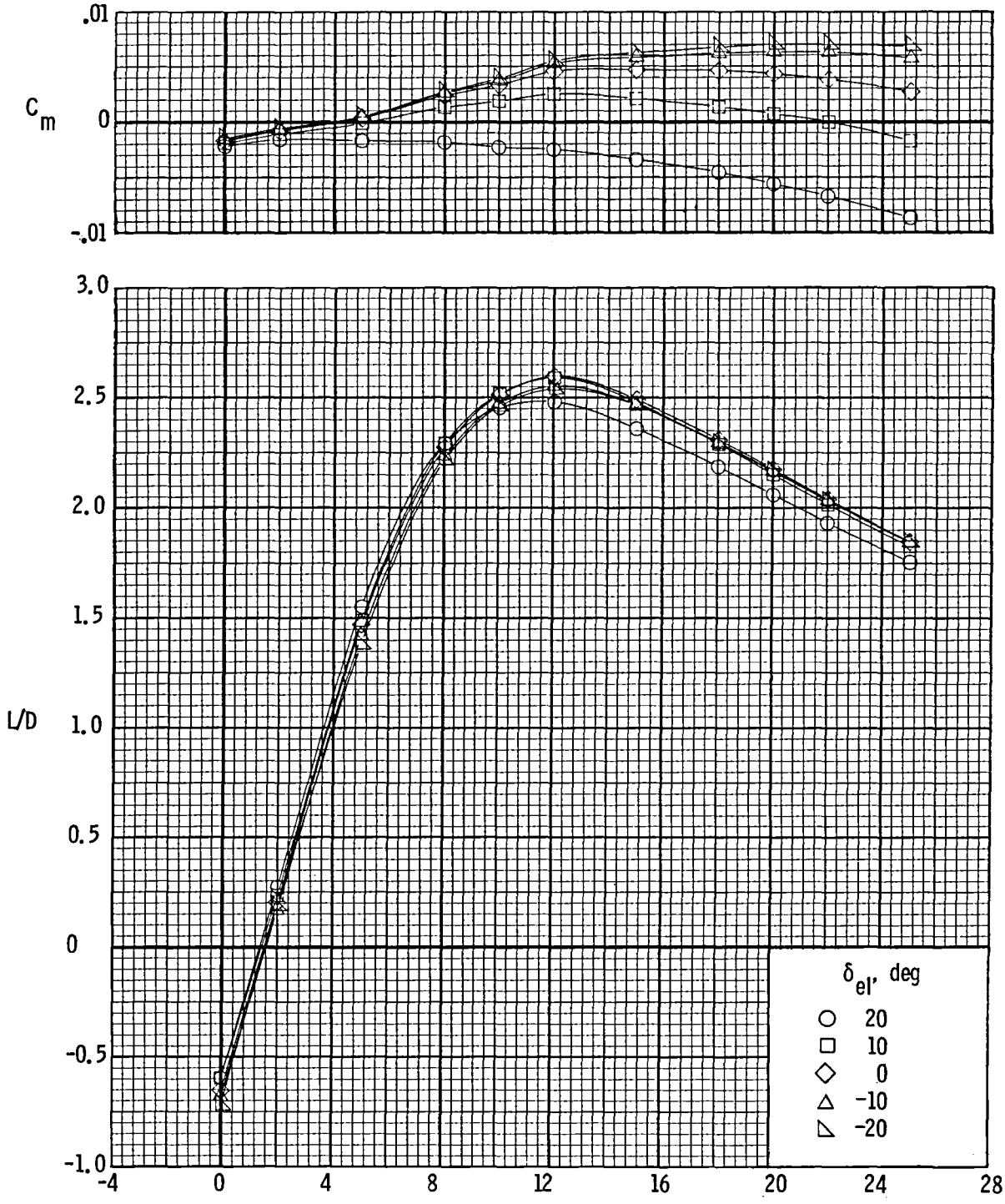

(a) C_m and L/D.

Figure 2.- Effects of elevator deflections on longitudinal characteristics. $R_\infty = 6.8 \times 10^6$ ft^{-1}; $\delta_e = 0°$.

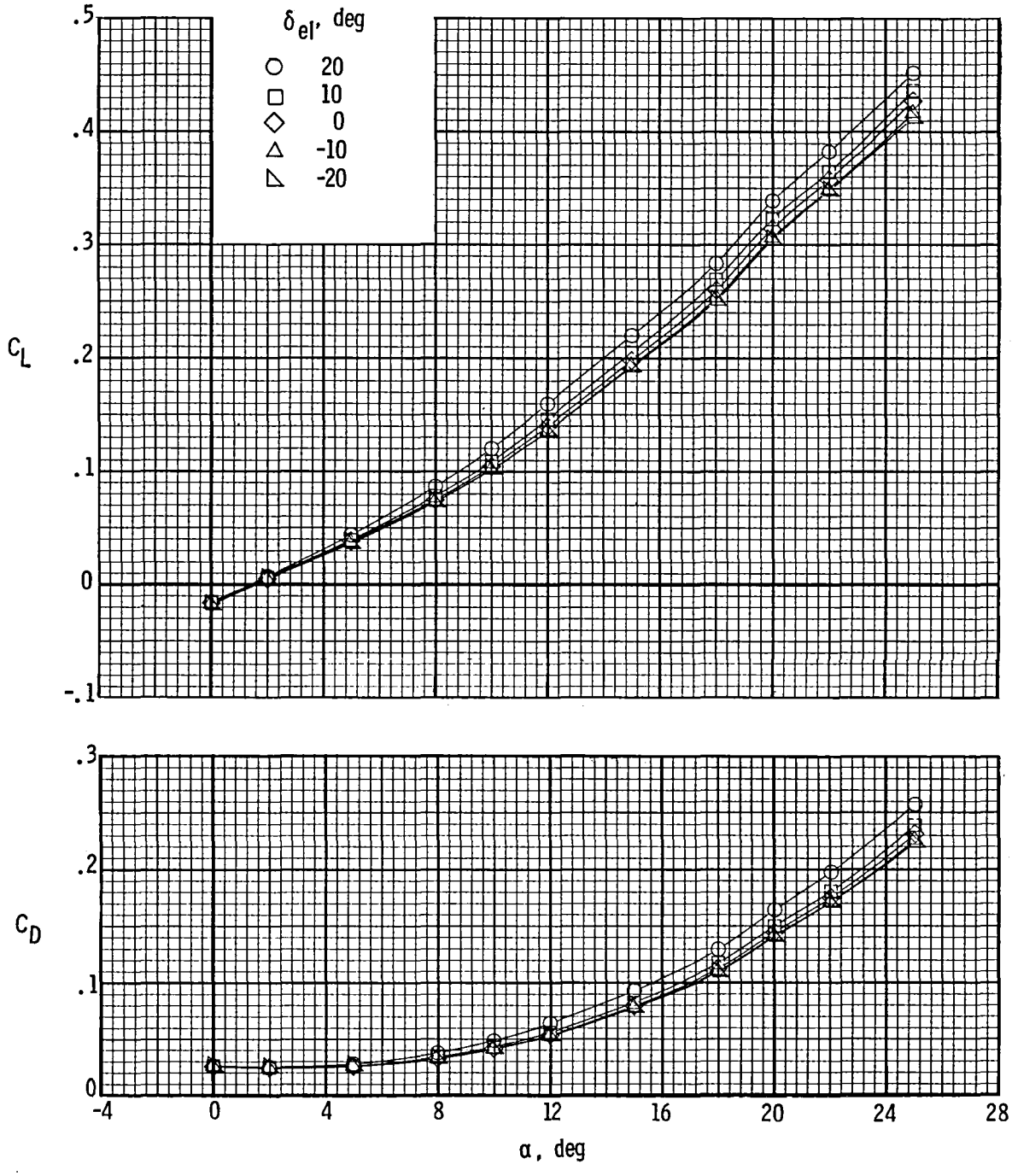

(b) C_L and C_D.

Figure 2.- Continued.

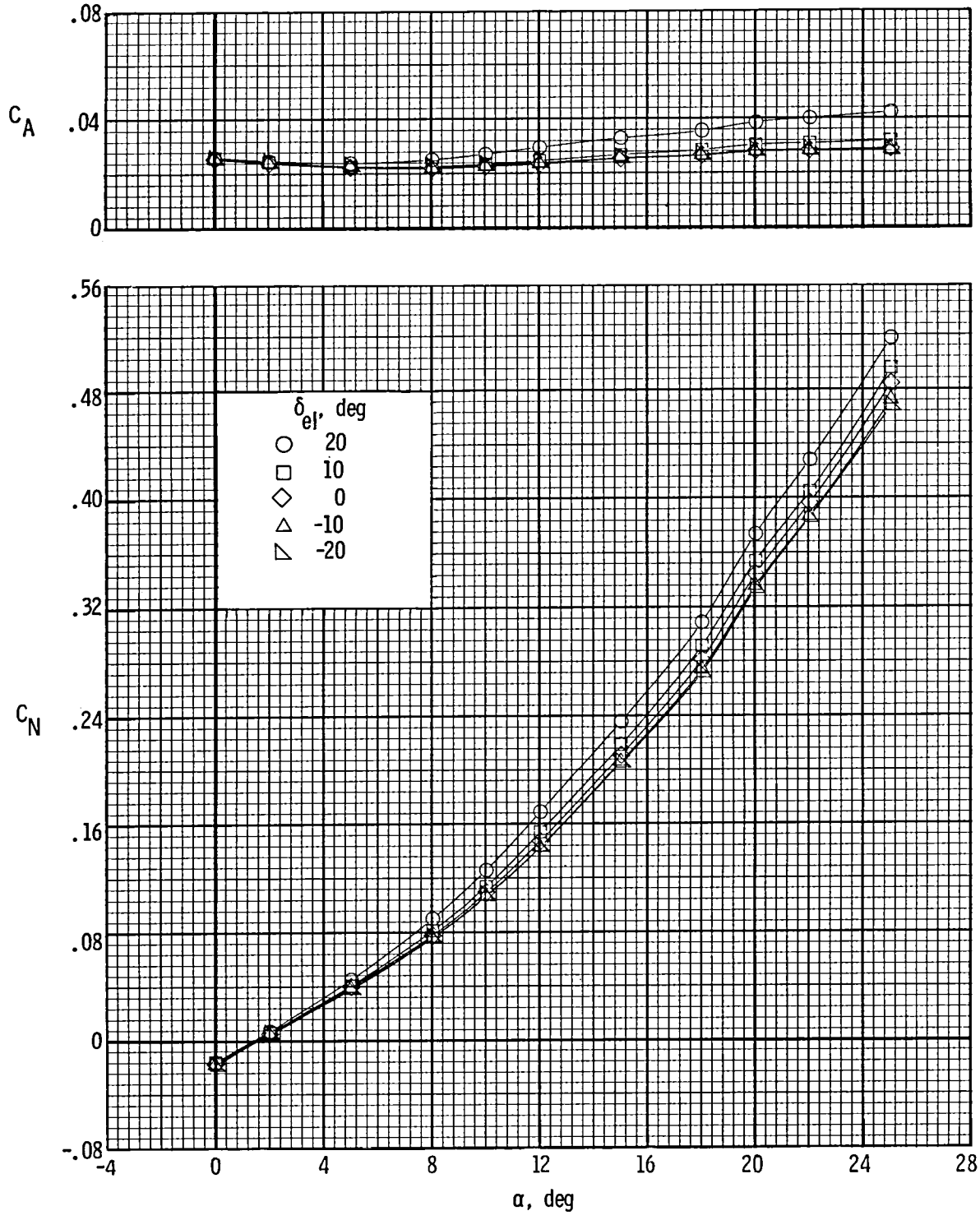

(c) C_A and C_N.

Figure 2.- Concluded.

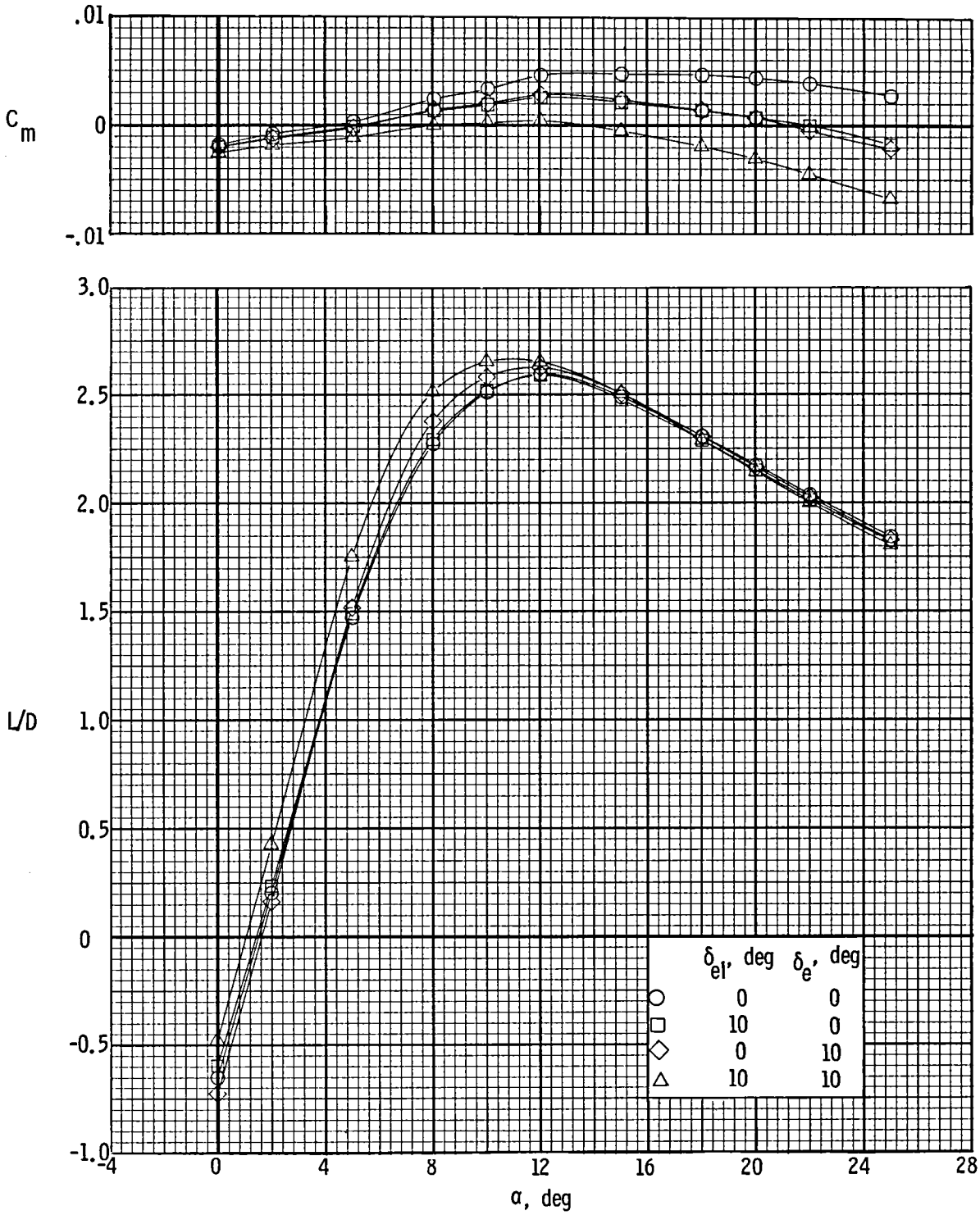

(a) C_m and L/D.

Figure 3.- Effects of elevon deflections on longitudinal characteristics. $R_\infty = 6.8 \times 10^6$ ft^{-1}; $\delta_r = 0°$.

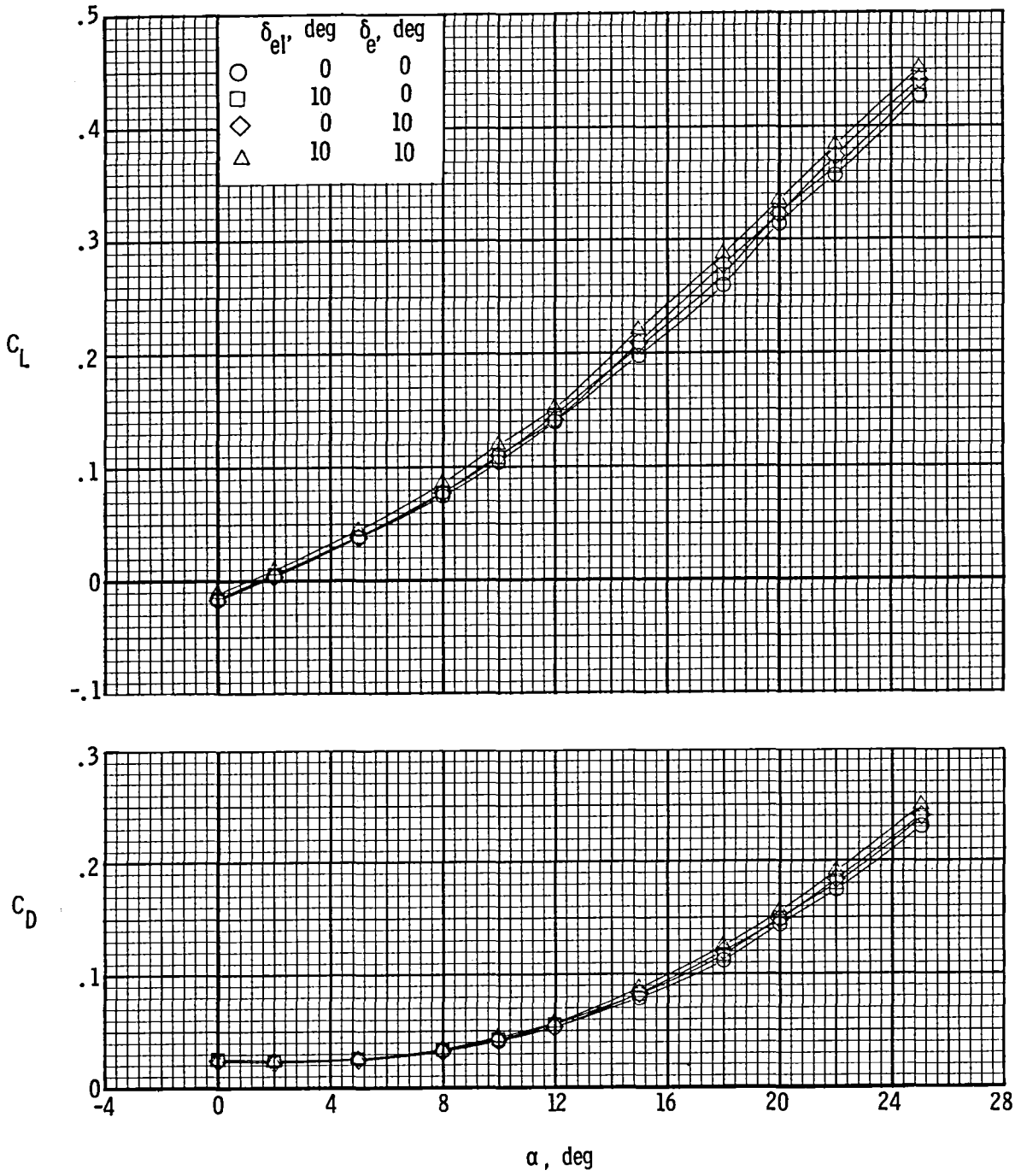

(b) C_L and C_D.

Figure 3.- Continued.

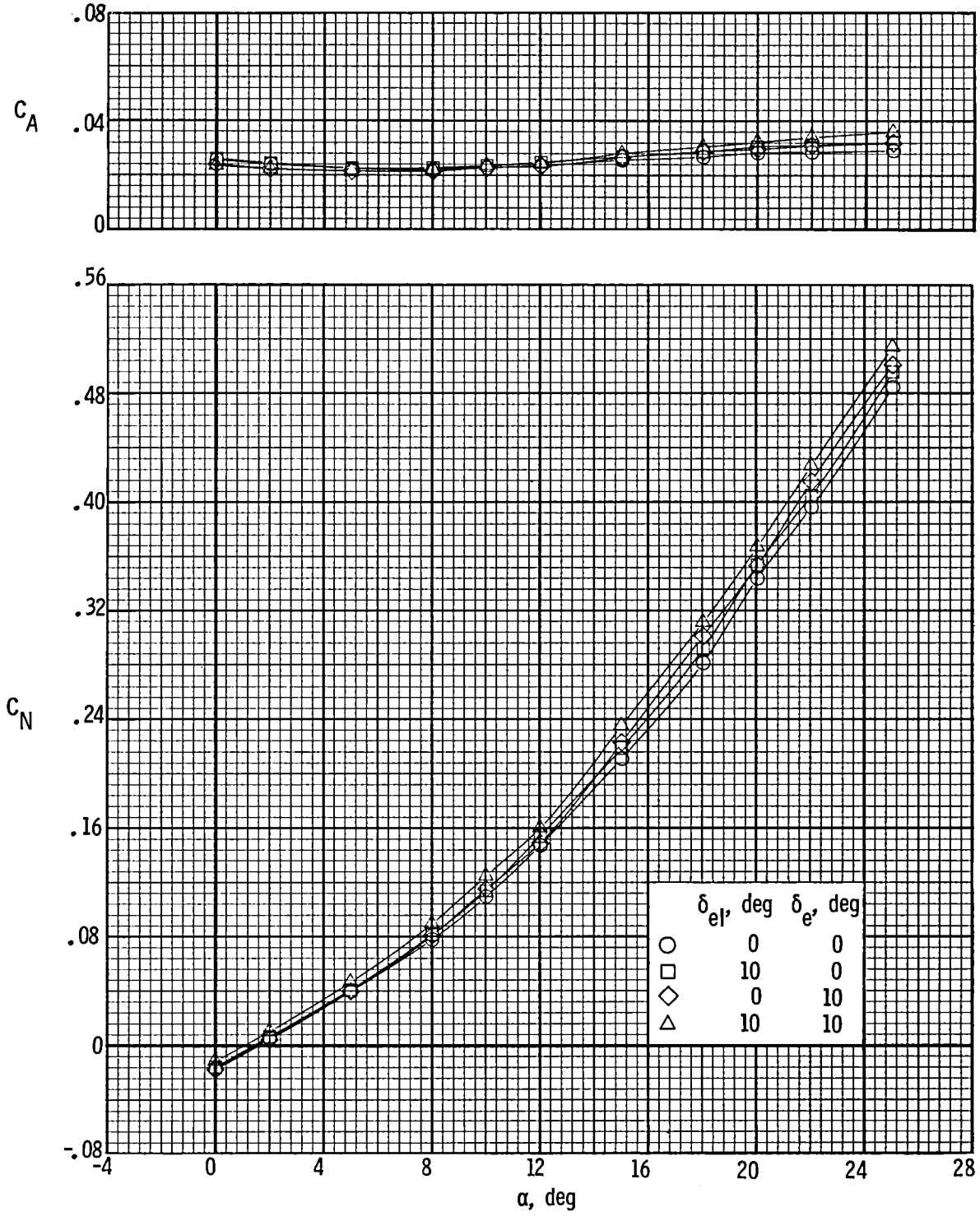

(c) C_A and C_N.

Figure 3.- Concluded.

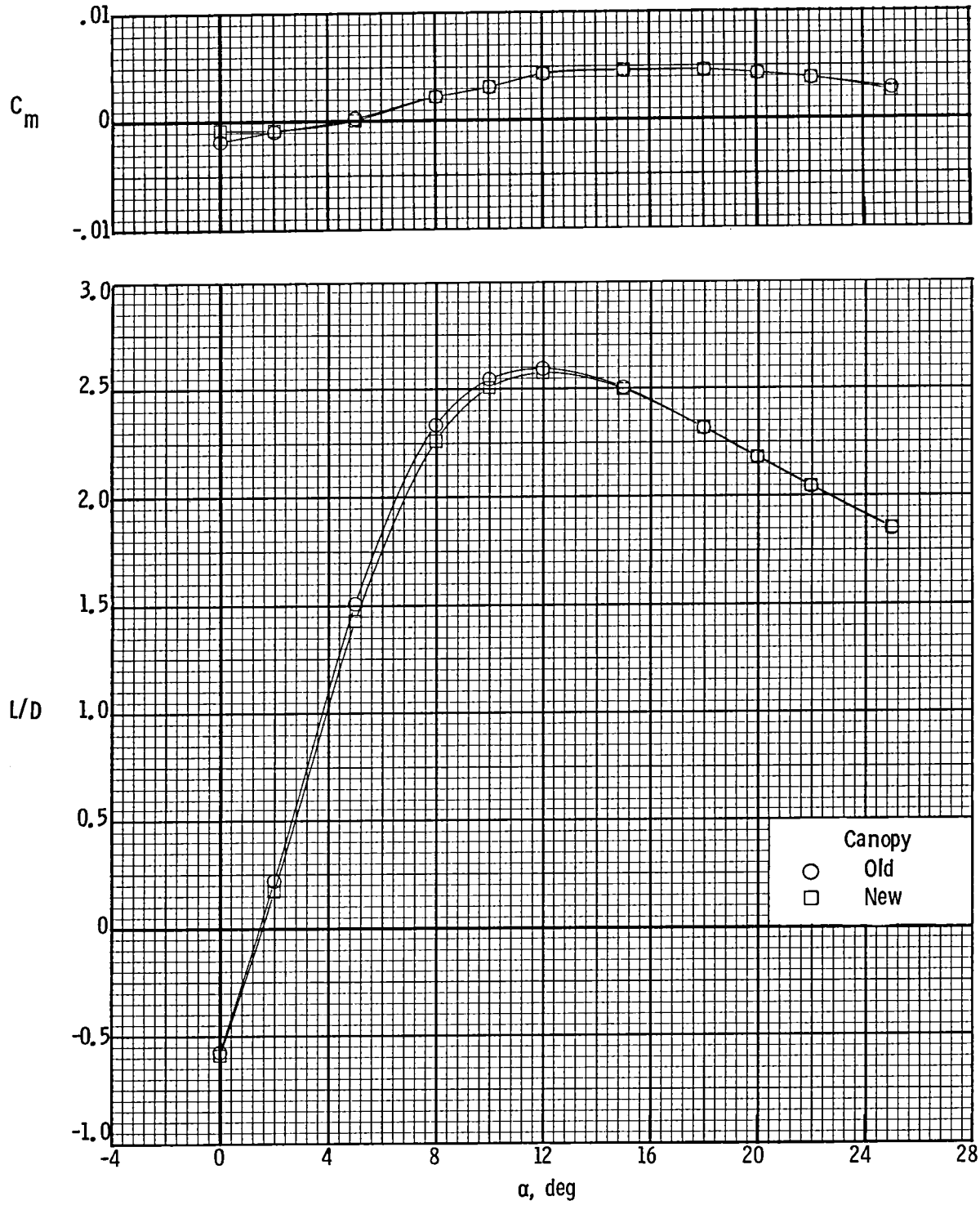

(a) C_m and L/D.

Figure 4.- Effects of modified canopy on longitudinal characteristics. $R_\infty = 6.8 \times 10^6$ ft^{-1}; $\delta_e = 0°$; $\delta_{el} = 0°$; $\delta_r = 0°$.

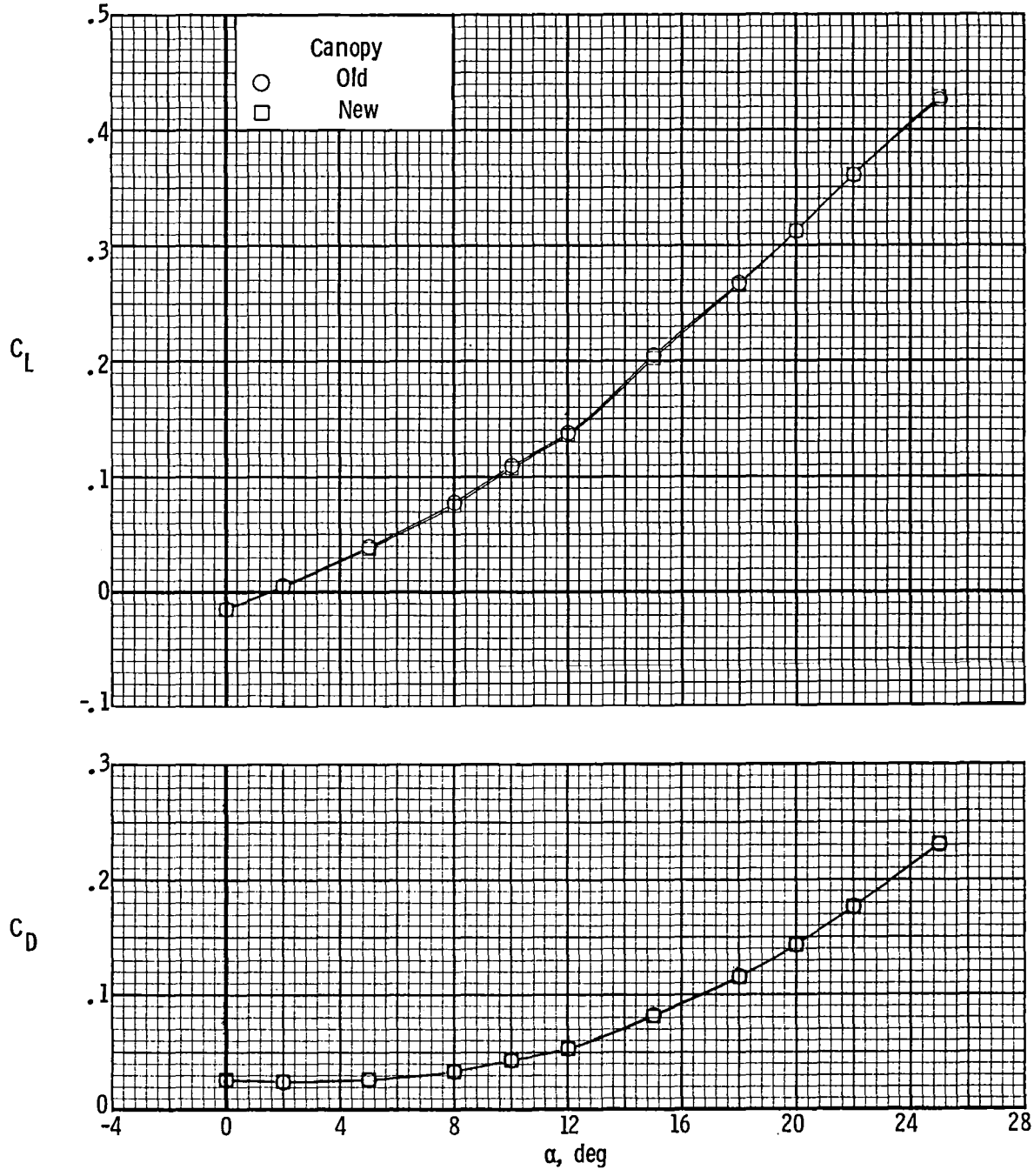

(b) C_L and C_D.

Figure 4.- Continued.

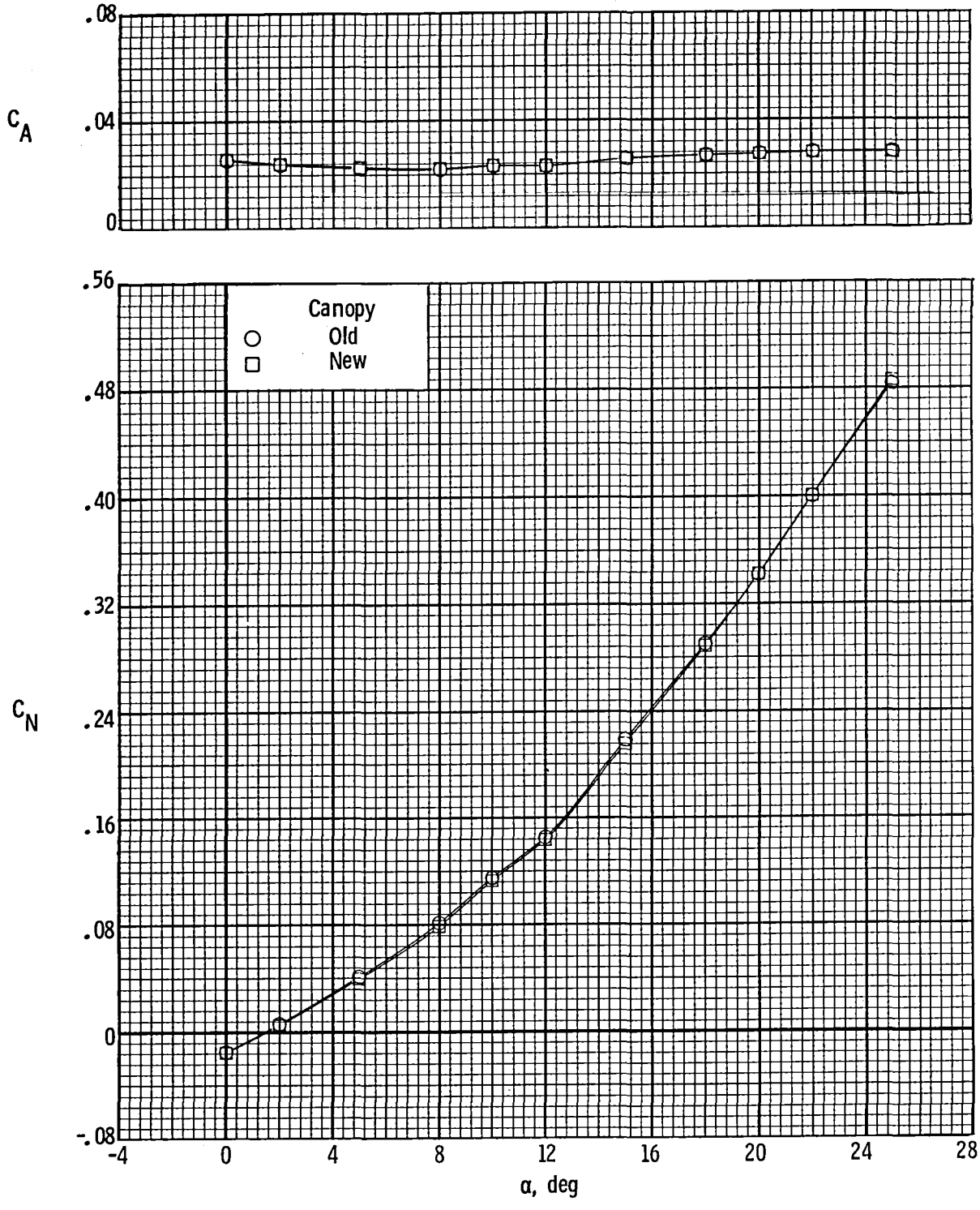

(c) C_A and C_N.

Figure 4.- Concluded.

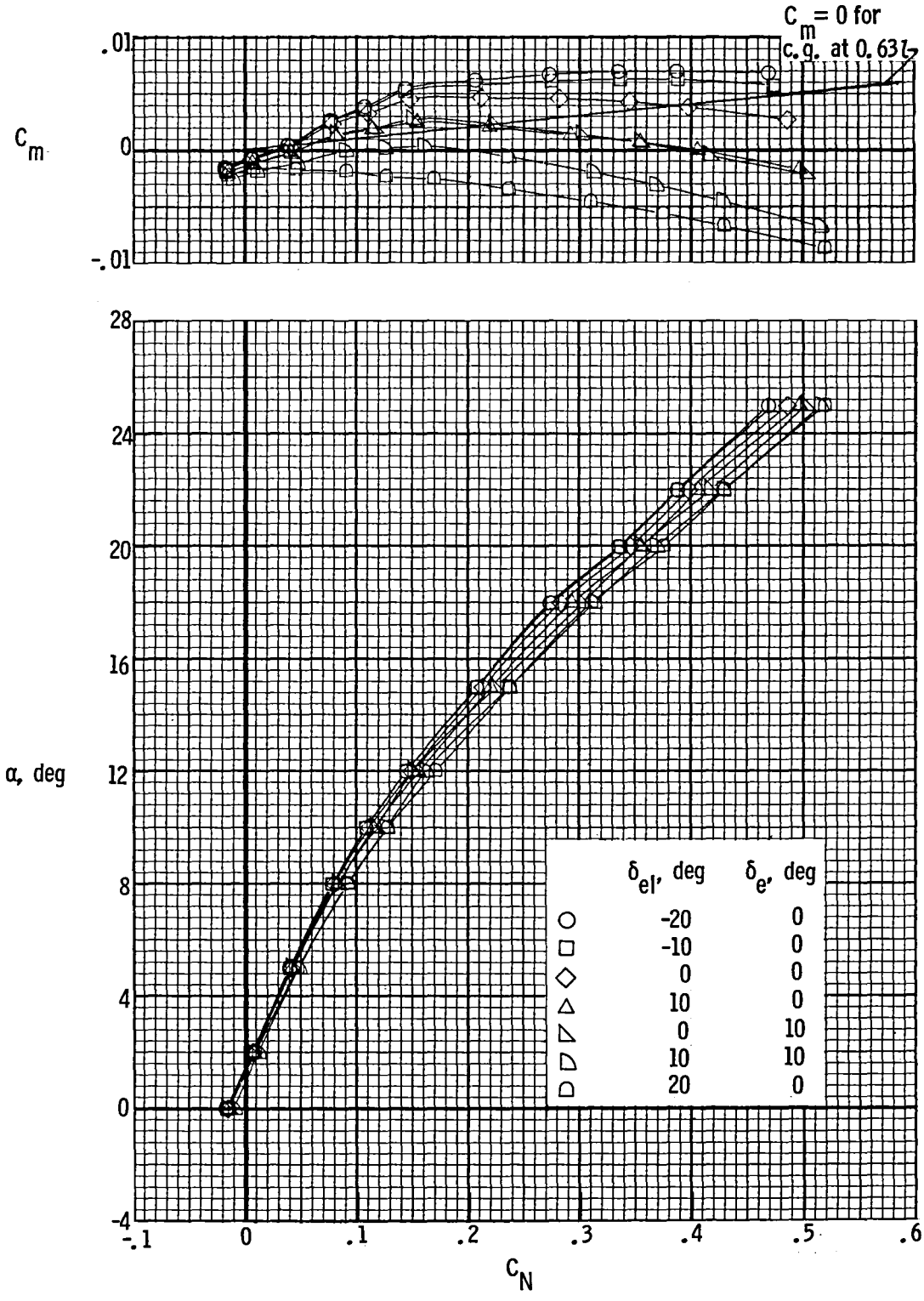

Figure 5.- Summary of effects of elevator and elevon deflections on longitudinal characteristics. $R_\infty = 6.8 \times 10^6$ ft^{-1}; $\delta_r = 0°$.

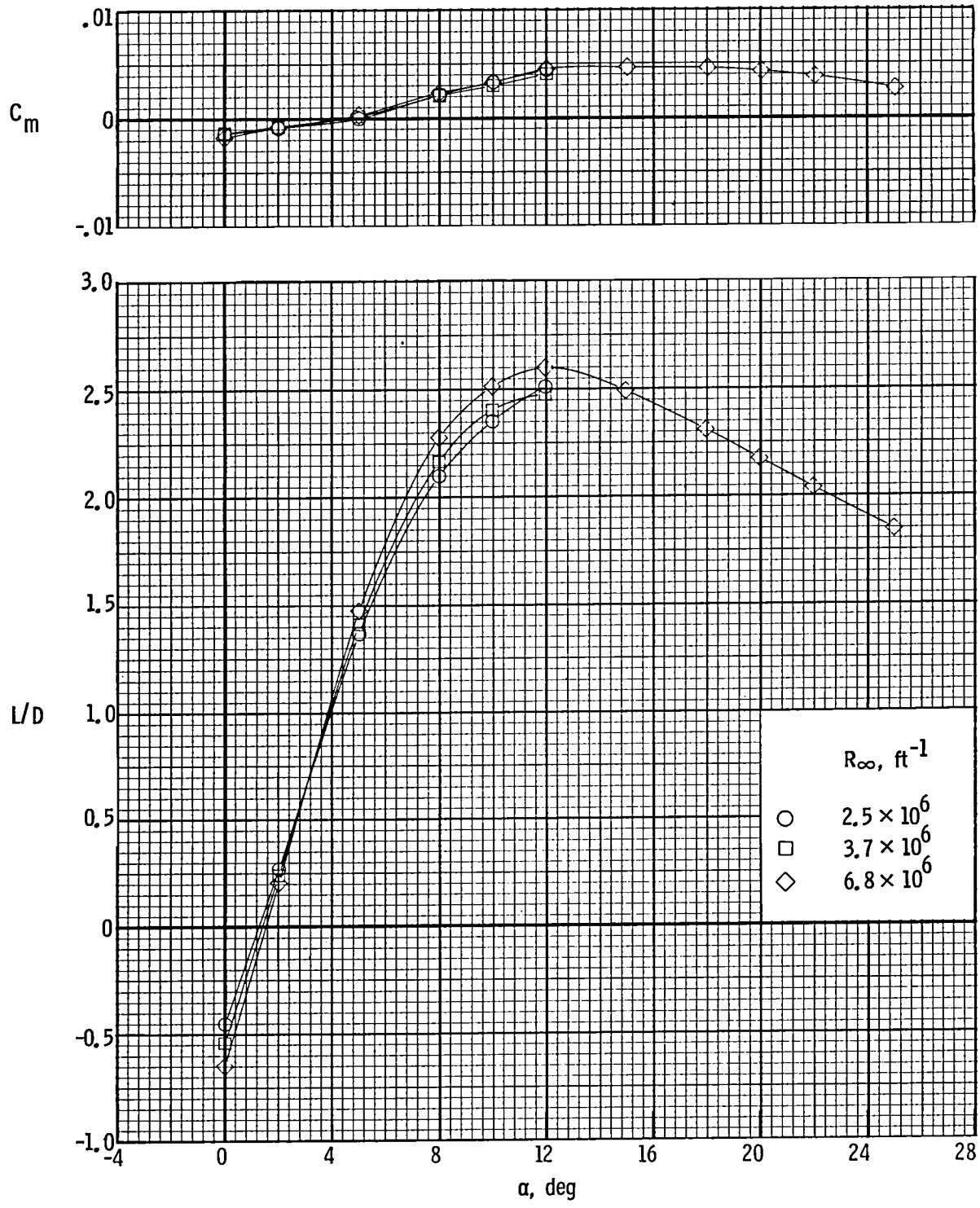

(a) C_m and L/D.

Figure 6.- Effects of Reynolds number on longitudinal characteristics. $\delta_{el} = 0°$; $\delta_e = 0°$; $\delta_r = 0°$.

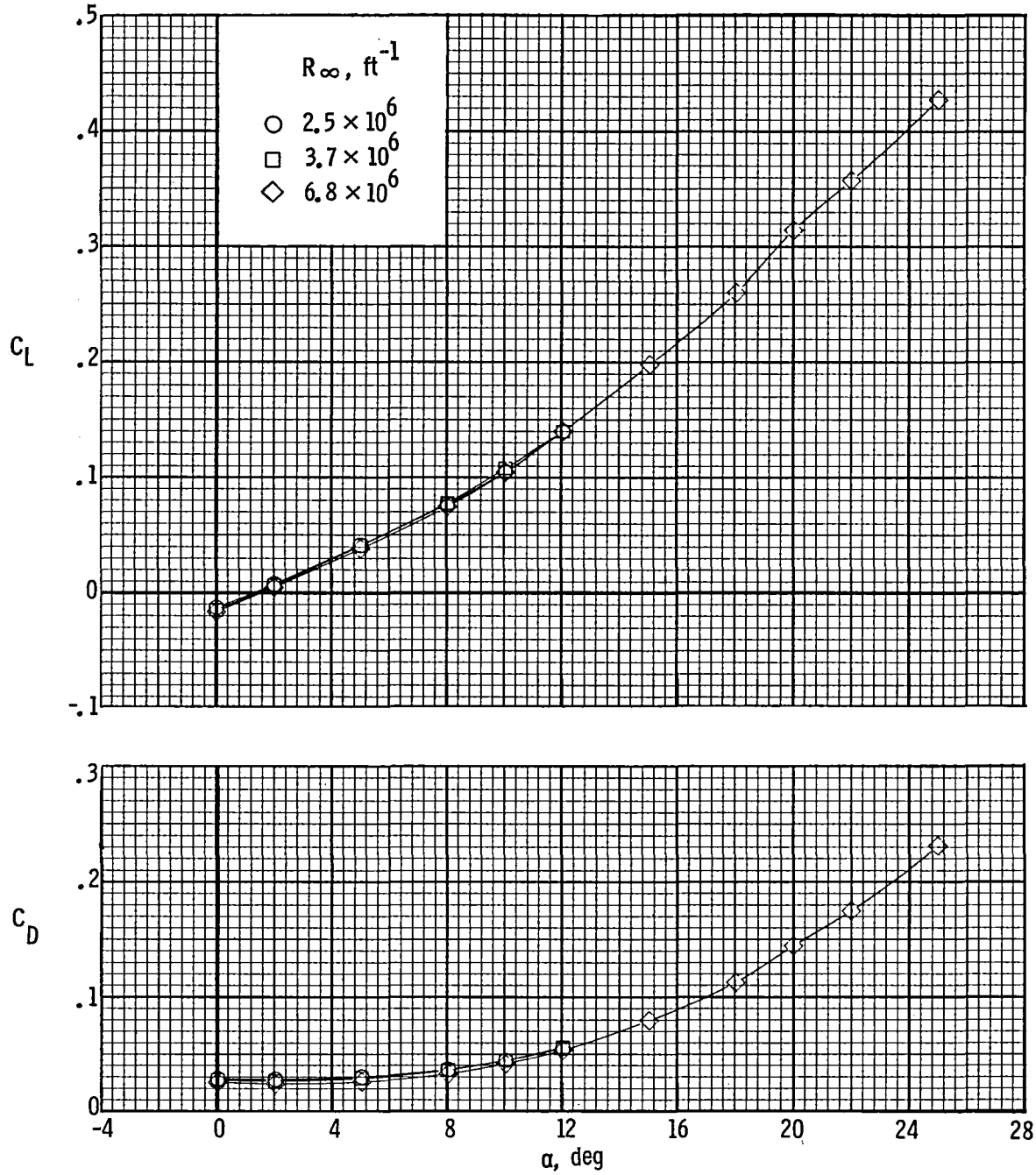

(b) C_L and C_D.

Figure 6.- Continued.

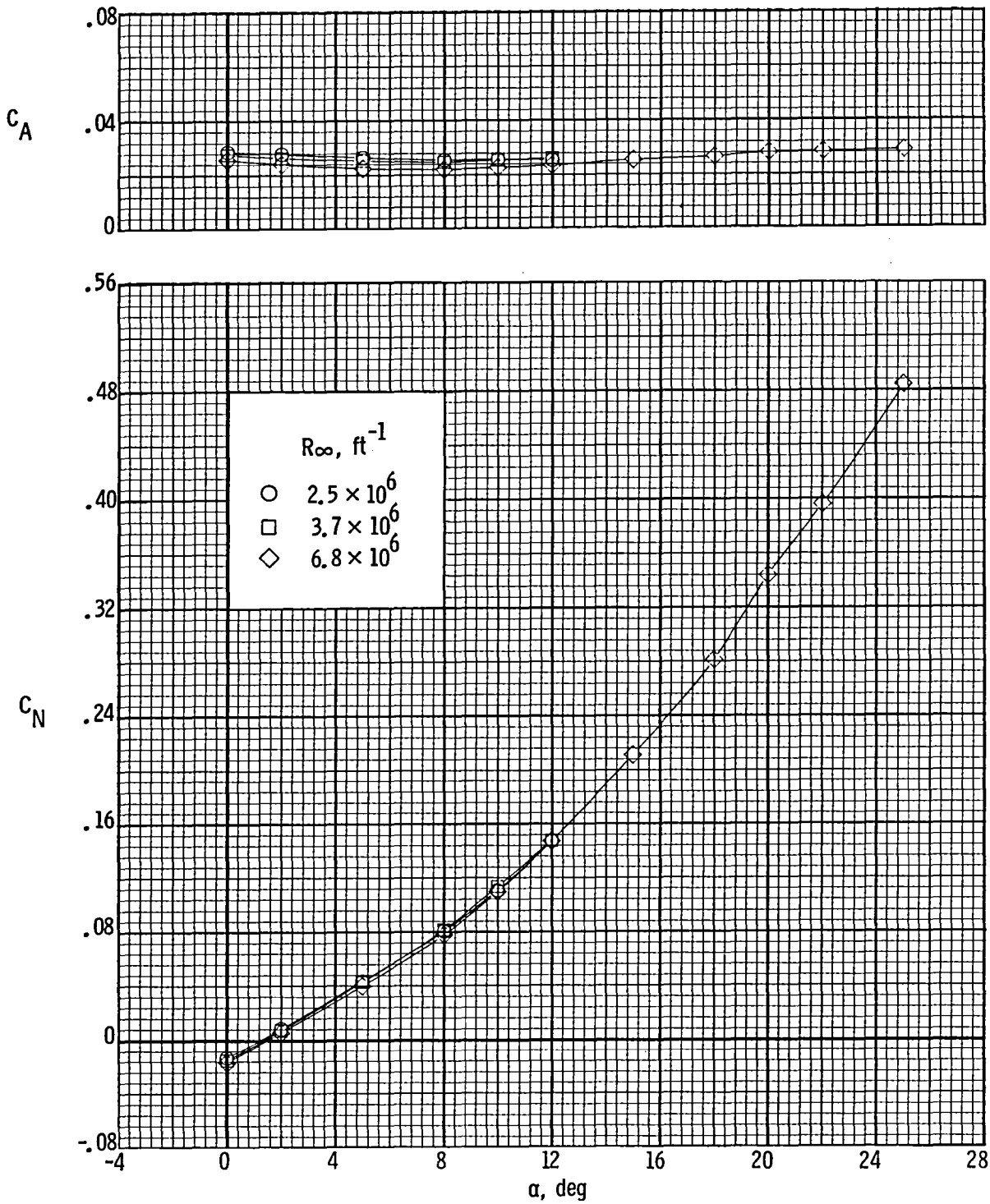

(c) C_A and C_N.

Figure 6.- Concluded.

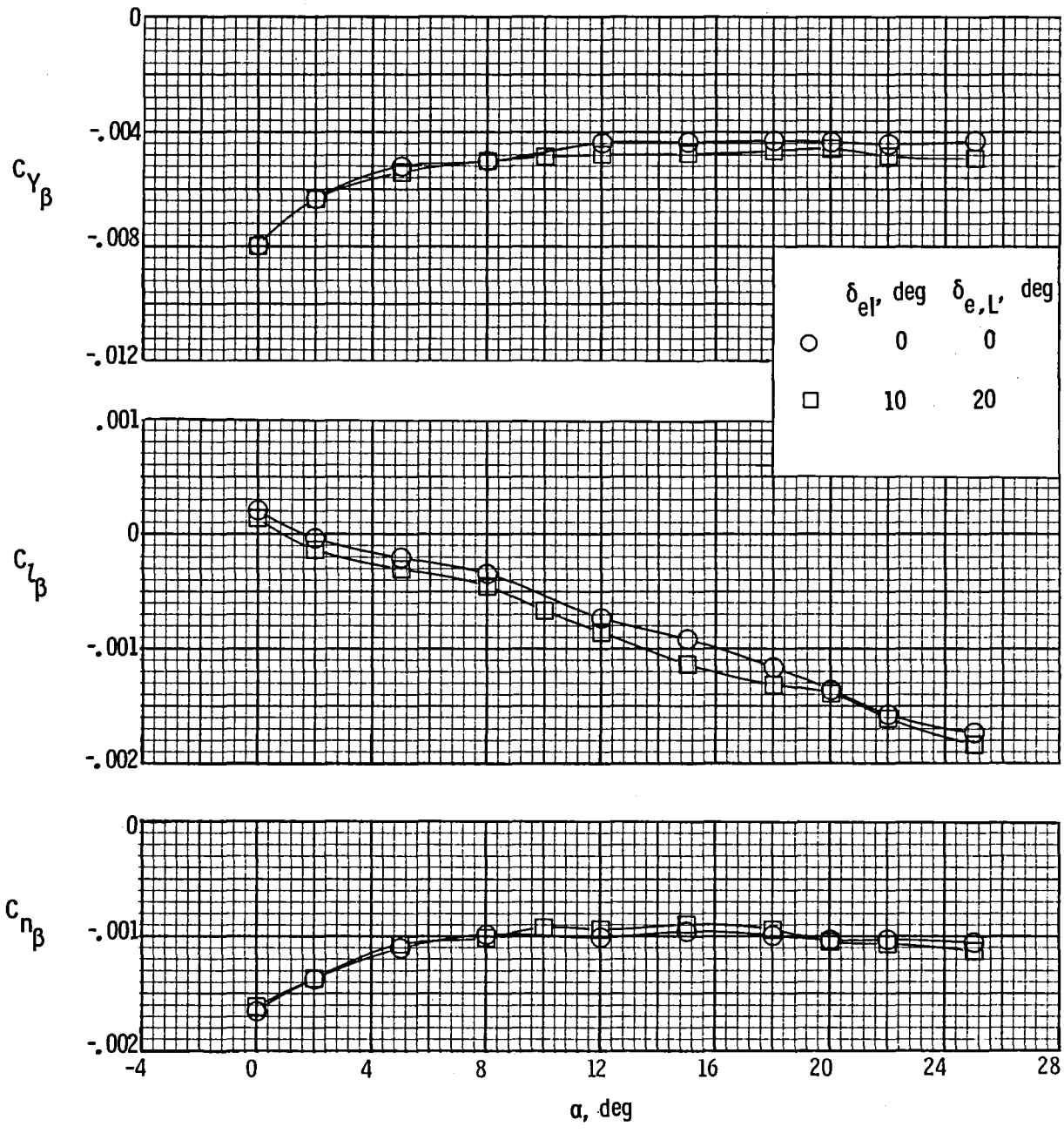

Figure 7.- Variation of lateral-directional derivatives with angle of attack for two cases. $R_\infty = 6.8 \times 10^6$ ft^{-1}; $\delta_{e,R} = 0°$.

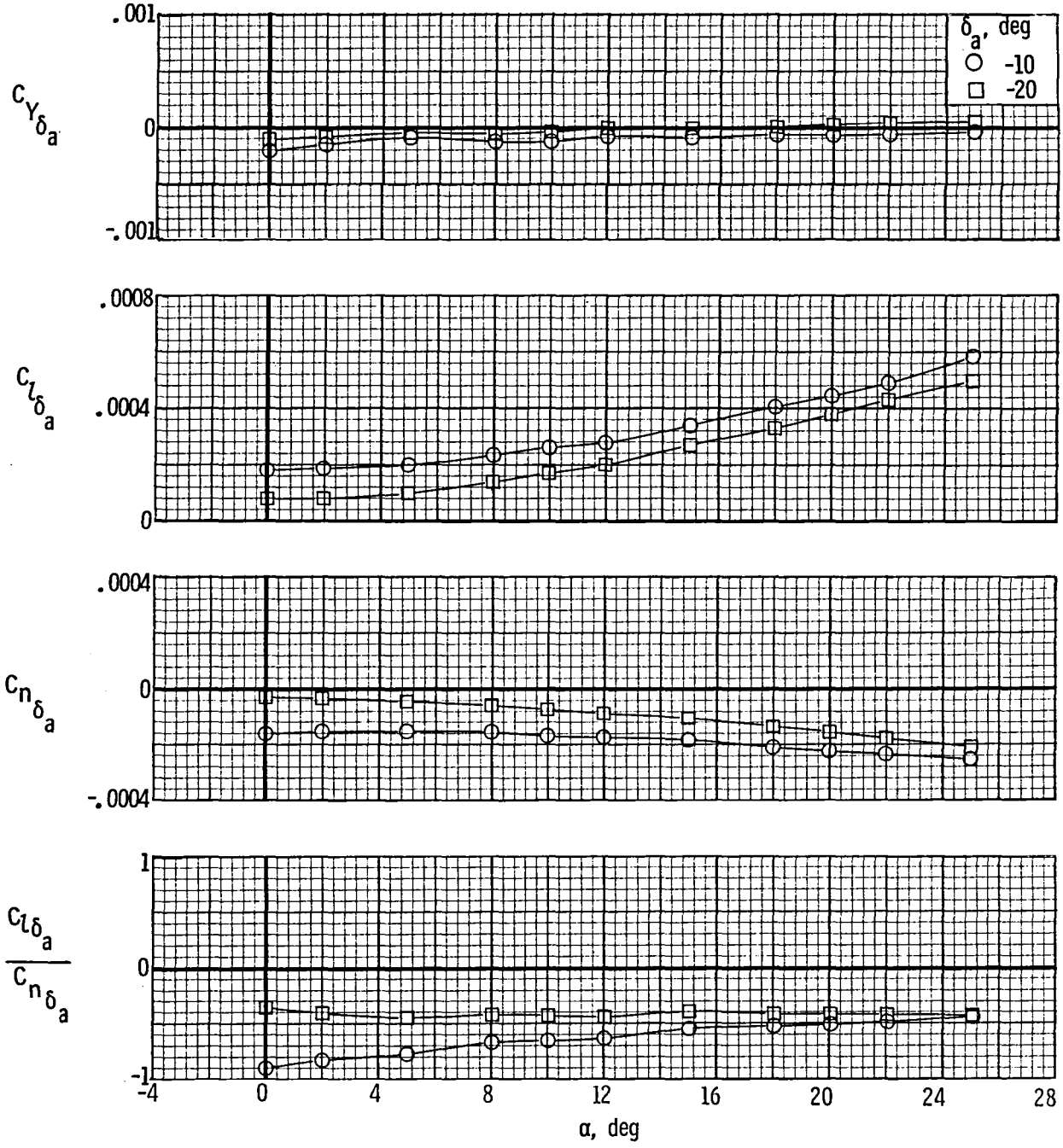

Figure 8.- Effects of aileron deflection on lateral-directional derivatives. $R_\infty = 6.8 \times 10^6$ ft^{-1}; $\delta_{el} = 0°$; $\delta_e = 0°$; $\delta_r = 0°$.

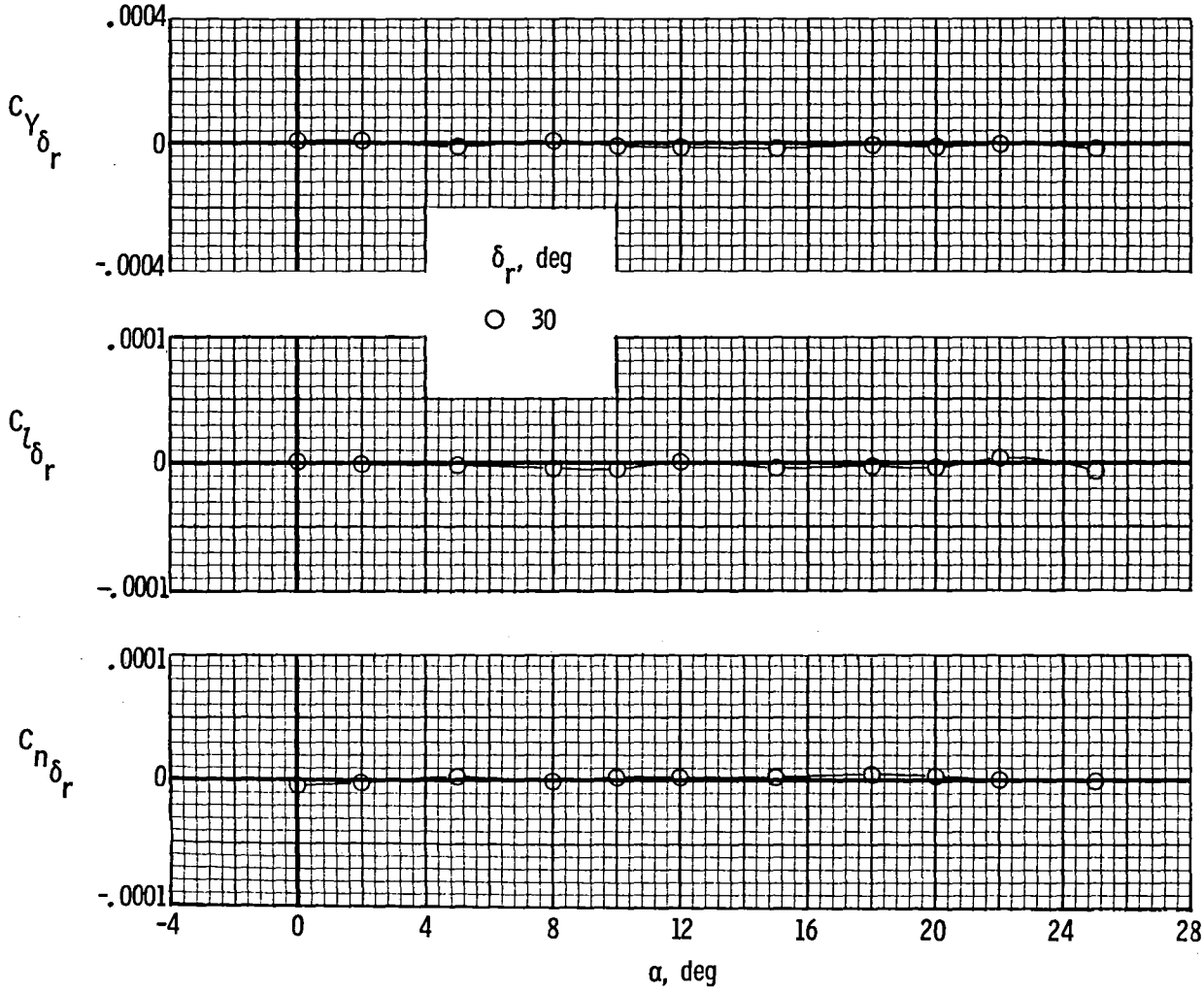

Figure 9.- Effects of rudder deflection on lateral-directional derivatives. $R_\infty = 6.8 \times 10^6$ ft^{-1}; $\delta_{el} = 0°$; $\delta_e = 0°$.

1. Report No.	2. Government Accession No.	3. Recipient's Catalog No.
NASA TM-86435		

4. Title and Subtitle	5. Report Date
Hypersonic Characteristics of an Advanced Aerospace Plane at Mach 20.3	December 1985
	6. Performing Organization Code: 506-51-13-02
7. Author(s): Ronald S. McCandless	8. Performing Organization Report No.: L-15953
9. Performing Organization Name and Address: NASA Langley Research Center, Hampton, VA 23665-5225	10. Work Unit No.
	11. Contract or Grant No.
12. Sponsoring Agency Name and Address: National Aeronautics and Space Administration, Washington, DC 20546-0001	13. Type of Report and Period Covered: Technical Memorandum
	14. Sponsoring Agency Code

15. Supplementary Notes

16. Abstract

Wind-tunnel studies have been performed in the Langley Hypersonic Helium Tunnel Facility to obtain static longitudinal and lateral-directional aerodynamic characteristics of an advanced aerospace plane concept. The nominal test conditions were a Mach number of 20.3 and a Reynolds number of 6.8×10^6 per foot at angles of attack from 0° to 25° and angles of sideslip of -3° and 0°. Stability and control characteristics were obtained for several deflections of the elevators, elevons, and rudder. In addition, a modified canopy was examined. The results indicate that this vehicle was longitudinally stable at angles of attack near the maximum lift-drag ratio. Also, the vehicle was shown to be directionally unstable with positive dihedral effect.

17. Key Words (Suggested by Authors(s))	18. Distribution Statement
Aerospace plane Aerodynamics	Unclassified - Unlimited Subject Categories 02, 15, 16

19. Security Classif.(of this report)	20. Security Classif.(of this page)	21. No. of Pages	22. Price
Unclassified	Unclassified	26	A03

For sale by the National Technical Information Service, Springfield, Virginia 22161

NASA-Langley, 1985

End of Document